MODAL PROPERTIES OF CROSS-FLOW INSTABILITY IN COMPRESSIBLE BOUNDARY LAYERS

Zhiyong Liu
Aerodynamics Science Center
China Academy of Aerospace Aerodynamics
No. 17 Yungang west road, Fengtai District, Beijing 100074, China
liuzhiyongtv@163.com

ABSTRACT

The present work is concerned with the stability characteristics of compressible boundary layers with crossflow on a flat plate. Based on a boundary-layer model on a flat plate, Linear Stability Theory (LST) is used to investigate the modal properties of cross-flow instability. The results reveal that asymmetry and negativeness of frequency are fundamental features for crossflow-affected instability, and two theorems are proposed to reveal the intrinsic details. Particularly, the conjugate mode is introduced to make the negative-frequency disturbance suitable for physical applications. In addition, the association between cross-flow mode and Mack's mode is clarified. It is found that the cross-flow instability is integrated with Tollmien-Schlichting (T-S) mode or the first mode, and it cannot be distinguished as a single mode for most cases.

INTRODUCTION

Crossflow is commonly encountered in three-dimensional (3-D) boundary layers, such as swept wings, yawed cones and high-speed flight vehicles with generally 3-D configurations. It is well accepted that the existence of inflection point often indicates an inviscid instability, which is usually called cross-flow instability. In most of the 3-D boundary layers, cross-flow instability co-exists with streamwise instabilities, like Tollmien-Schlichting (T-S) waves and Mack's modes. While in contrast with streamwise instabilities, cross-flow instability exhibits unstable disturbances that are traveling as well as stationary. Linear Stability Theory (LST) shows larger amplification rates for the traveling modes than the stationary ones. Concerning the crossflow-induced boundary-layer transition, however, stationary waves play an important role in low-turbulence environments, while the traveling waves dominate in high-turbulence environments (Saric, Reed & White 2003).

Increasing understanding of cross-flow instability has been achieved in past decades in experiments and numerical simulations. Nevertheless, some common and fundamental issues about cross-flow instability still need to be figured out. Firstly, both the cross-flow mode and Mack mode exist in compressible 3-D boundary layers, whereas the association and difference have not been elucidated. The boundary-layer stability analyses on a yawed cone (Li *et al*. 2016) and an elliptic cone (Paredes *et al*. 2016) indicated distinct features between cross-flow instability and Mack's second-mode instability. However, the comparison between the evolvements of slow mode in 2-D (Ma & Zhong 2005) and 3-D (Xu *et al*. 2018) compressible boundary layers implies some connection existing between cross-flow mode and Mack mode. Secondly, it is not well understood that how do the stability characteristics change when crossflow plays a role in a 3-D boundary layer. Specifically, the changes of interest include quantitative variations of growth rate, unstable region and dominance of different instabilities with increasing strength of crossflow in base flow.

Such understanding about primary instability sheds light on the research of receptivity (Schrader, Brandt & Henningson 2009; Balakumar & King 2012; Xu *et al*. 2018), secondary instability (Högberg & Henningson 1998; Malik *et al*. 1999; Xu *et al*. 2019) and flow control (Wassermann & Kloker 2002; Schuele, Corke & Matlis 2013; Corke *et al*. 2018) of cross-flow instability-dominated boundary layers. Numerical simulations (Pruett, Chang & Streett 2000; Dinzl & Candler 2017) and experimental tests (White & Saric 2005; Craig & Saric 2016) have benefited from the theoretical studies as well.

Nevertheless, some common and fundamental issues about cross-flow instability still need to be figured out. Firstly, both the cross-flow mode and Mack mode exist in compressible 3-D boundary layers, whereas the association and difference have not been elucidated. The boundary-layer stability analyses on a yawed cone (Li *et al*. 2016) and an elliptic cone (Paredes *et al*. 2016) indicated distinct features between cross-flow instability and Mack's second-mode instability. However, the comparison between the evolvements of slow mode in 2-D (Ma & Zhong 2005) and 3-D (Xu *et al*. 2018) compressible boundary layers implies some connection existing between cross-flow mode and Mack mode. Moreover, the relationship between traveling cross-flow mode and Mack's first mode has not been addressed, despite that the frequency band of the two modes overlaps largely. Similar situation exists as well for traveling cross-flow mode and T-S mode in low-speed boundary layers. Secondly, it is not well understood that how do the stability characteristics change when crossflow plays a role in a 3-D boundary layer. Specifically, the changes of interest include quantitative variations of growth rate, unstable region and dominance of different instabilities with increasing strength of crossflow in base flow. Perhaps the most striking phenomenon caused by crossflow is the occurrence of zero- and negative-frequency cross-flow modes, in which the zero-frequency (stationary) one was proved to be crucial to secondary instability and nonlinear interactions (Malik, Li & Chang 1994; Malik *et al*. 1999; Pruett, Chang & Streett 2000; Craig & Saric 2016). The critical value, if it exists, of crossflow to induce cross-flow mode with non-positive frequency has not been unraveled yet. Thirdly, significance and characteristic of negative-frequency cross-flow mode have not been demonstrated in detail. Cross-flow instability with negative-frequency region has been discovered for long (Mack 1984; Högberg & Henningson 1998; Itoh 1996). Mack (1984) pointed out that the opposite sign of frequency indicated opposite propagation directions of disturbances, which was consistent with the statement of Itoh (1996). However, the interpretation about negative-frequency mode is not in direct accordance with the eigen solution of LST equations. More details need to be disclosed to support a more satisfactory explanation.

In addition, in order to shed some light on the general characteristics of cross-flow instability, analyses are made under different Mach numbers, Reynolds numbers and temperature boundary conditions. However, systematic knowledge of cross-flow instability can hardly be obtained from case-by-case investigations aforementioned. Mack (1984) presented a comprehensive study of the linear stability of 2-D compressible boundary layers, based on the mean flow with an exact solution. While for 3-D compressible boundary layers, the counterpart research has been substantially hindered due to lacking a simplified solution of laminar base flow. Therefore, an appropriate boundary-layer solution needs to be obtained to initiate the comprehensive stability analysis of cross-flow instability.

Following the research paradigm of Mack (1984), we developed a model problem for compressible boundary layers with parametric crossflow to study the linear instabilities due to the presence of typical crossflow. The main purpose of present work is to illustrate some fundamentals of cross-flow instability and to clarify how it associates with the instability modes already known in 2-D boundary layers.

BASE FLOW

A model problem for compressible boundary layer is established on an infinite flat plate (Fig. 1). The Cartesian coordinate system is set up as follows. The *y* direction points normal to the plate. Pressure gradient is equipped in parallel with the plate. The direction of pressure gradient is designated as *x* direction in Cartesian coordinate system, and the pressure gradient occupies the area over the plate. The *z* direction points normal to the *x*-*y* plane. The incoming flow consists of two velocity components in *x* and *z* directions, respectively. Depending on favorable or adverse pressure gradient, the inviscid potential flow accelerates or decelerate in *x* direction on the plate, while the *z*-direction velocity keeps unchanged. The pressure gradient in misalignment with velocity direction curves the inviscid streamlines over the flat plate. Similar flow configuration was used to study cross-flow instabilities in incompressible (Wassermann & Kloker 2003) and compressible (Tempelmann, Hanifi & Henningson 2012; Xu *et al*. 2018) conditions.

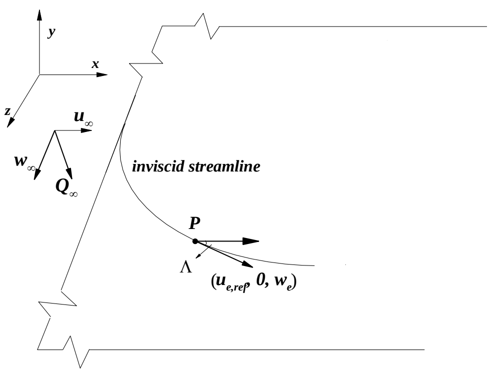

Figure 1. The Cartesian coordinate system on a semi-infinite flat plate. The local swept angle Λ denotes the angle between directions of velocity and pressure gradient in potential flow. The subscripts '∞', '*e*' and '*ref*' represent incoming flow, boundary-layer edge and reference point, respectively.

For the infinite conditions in *z* direction, the variables of the steady laminar base flow are independent of *z*. Reference point P is appointed at $x=x_{ref}$, where the local flow is concerned. The base flow is governed by quasi-three-dimensional compressible boundary-layer equations. By introducing stream function and Illingworth-Stewartson transformation, and assuming Falkner-Skan external potential flow in *x* direction, we obtain an ordinary-differential-equation (ODE) system under local-similarity assumption (Liu, 2021).

$$\left(Nf''\right)' + ff'' = \frac{2m}{(m+1)S}\left(f'^2 - \tau\right), \tag{1}$$

$$\left(Ng'\right)' + fg' = 0, \tag{2}$$

$$\left(\frac{N}{Pr}\tau'\right)' + (S-1)\left(N\left(f'^2\right)'\right)' + (K-1)S\left(N\left(g^2\right)'\right)' \tag{3}$$
$$+ f\left(\tau' + (S-1)\left(f'^2\right)' + (K-1)S\left(g^2\right)'\right) = 0.$$

Boundary conditions are written as

$$\eta = 0: \quad f = f' = g = 0, \quad \tau = \tau_w \quad or \quad \tau' = 0, \tag{4}$$

$$\eta \to \infty: \quad f' = g = \tau = 1. \tag{5}$$

Based on the solution of the ODE system, the streamwise and crosswise velocity components can be written as

$$u = \frac{L^2 f' \cos^2\Lambda + g\sin^2\Lambda}{L^2\cos^2\Lambda + \sin^2\Lambda}, \tag{6}$$

$$w = \frac{L\left(g - f'\right)\cos\Lambda\sin\Lambda}{L^2\cos^2\Lambda + \sin^2\Lambda}. \tag{7}$$

Such flow model is named Falkner-Skan-Cooke(FSC) boundary layer. The crossflow distributions under different flow parameters are displayed in Fig. 2. The influence of local swept angle on crossflow in an incompressible boundary layer is demonstrated in Fig. 2(a). The crossflow deviates from zero and gets stronger with the increase of local swept angle until a largest maximum is reached on the profile. The largest maximum of crossflow occurs precisely at $\Lambda=45^{\circ}$. In addition, the distributions of crossflow under two swept angles, which are mutually complementary, are identical. However, slightly different results appear in compressible boundary layers, where the largest maximum occurs at around $\Lambda=70^{\circ}$ and no special relations are observed for different local swept angles (Fig. 2(b)). Pressure-gradient parameter affects the crossflow both in magnitude and direction, as shown in Fig. 2(c). Favorable pressure gradients produce positive crossflow components, while adverse pressure gradients act otherwise. Meanwhile, for positive values of m, it is observed that pressure gradient with larger magnitude produces stronger crossflow but thinner boundary layer. Lastly in Fig. 2(d), wall cooling is found to weaken the crossflow as well as thin the boundary layer.

The crossflow exhibits a variety of profiles under different combinations of flow parameters, which provides rich diversity of base flow. Corresponding variations of crossflow-induced stability characteristics are expected to appear in the 3-D boundary layers.

The crossflow in current model is controlled by pressure-gradient parameter *m* and local swept angle Λ. On the one hand, when the local swept angle vanishes, the system is reduced to the one describing a 2-D compressible boundary layer with self-similarity (Stewartson 1964). On the other hand, when Mach number approaches zero, the system is reduced to the Falkner-Skan-Cooke flow describing an incompressible 3-D boundary layer (Cooke 1950). Therefore, the well-known stability characteristics in classical boundary layers can be extended to 3-D compressible conditions with the aid of current base-flow model.

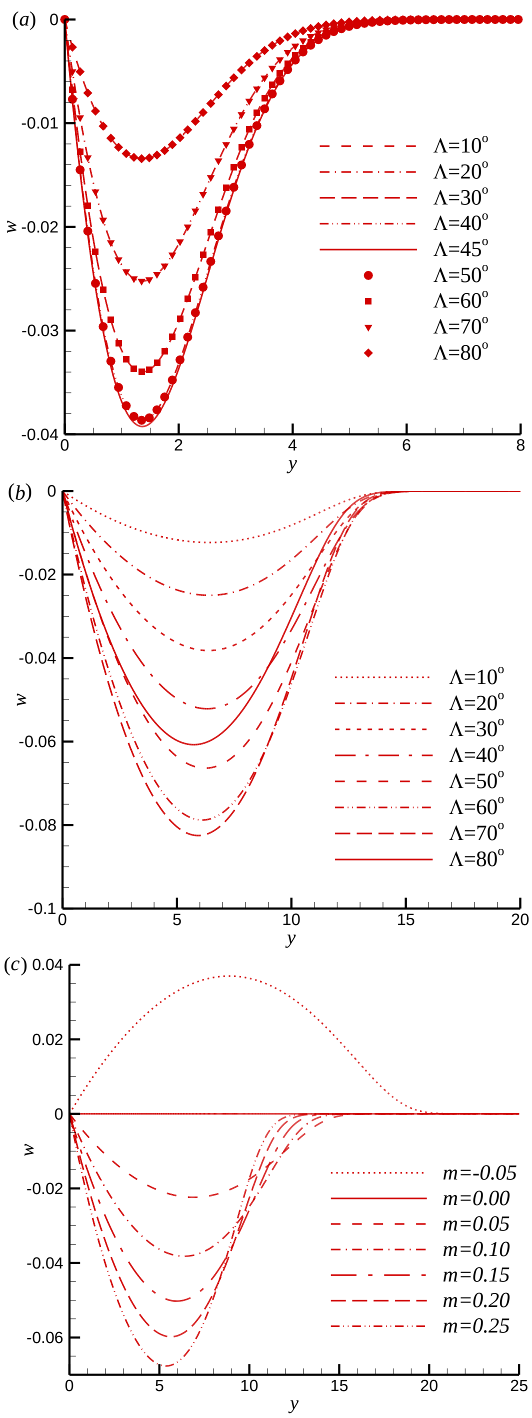

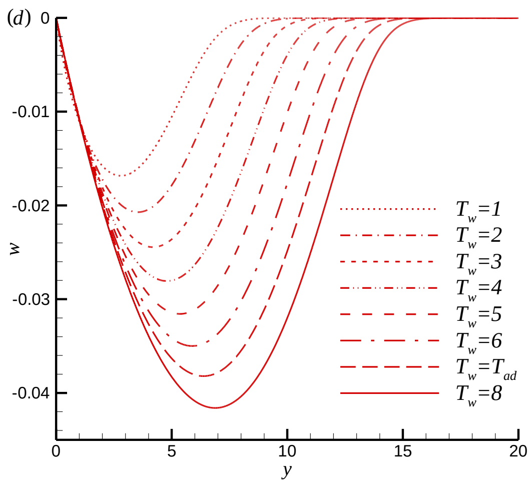

Figure 2. Variations of cross-flow profile with (*a*) local swept angle at *Ma*=0.001 (*m*=0.1), (*b*) local swept angle at *Ma*=6.0 ($T_w=T_{ad}$, *m*=0.1), (*c*) pressure-gradient parameter at *Ma*=6.0 ($T_w=T_{ad}$, $\Lambda=30^o$) and (*d*) wall temperature at *Ma*=6.0 (*m*=0.1, $\Lambda=30^o$). $T_w\approx7.0$ for an adiabatic wall in this case.

LINEAR STABILITY THEORY

The modal properties of boundary-layer instabilities are analyzed with LST, which is well known and introduced in quite a lot literatures, say Mack (1984). Two facts are presented as theorems to elaborate the characteristics of crossflow-related instability. The proofs of the two theorems are straightforward, thus not presented here.

The *Conjugate-Solution Theorem* is stated as below.

Given $(\omega,\alpha,\beta,\phi)$ *as the solution of LST equation, the conjugate solution* $(-\hat{\omega},-\hat{\alpha},-\hat{\beta},-\hat{\phi})$ *exists.*

$\hat{\alpha}$ denotes the conjugate of α, and so do $\hat{\omega}$ and $\hat{\phi}$. The related solution is named conjugate solution, or conjugate mode to each other. Considering all of the parameters as complex, it can be seen that the conjugate solution of $(\omega,\alpha,\beta,\phi)$ is actually the negative and conjugate combination. Therefore, when a mode with positive frequency is found, there must exist a negative counterpart, and vice versa. Based on such association, a negative-frequency disturbance, which might be deficient in physical significance, relates to a positive-frequency disturbance with opposite wave-number vector and equal growth rate ($-\alpha_i$). This provides alternative interpretation for the disturbance with negative frequency. By revisiting Mack's assertion, it can be concluded that the negative frequency indeed signifies propagation-direction reversal of disturbance, which, however, corresponds to a different eigen solution. LST results about conjugate mode are demonstrated in next section. It should also be noted that the fact about conjugate mode holds for linear stability in all parallel flows, as long as equation and boundary conditions are homogeneous.

Compared with 2-D flows, three-dimensionality of base flow in 3-D flows gives rise to deviation of stability characteristics. Different from the three-dimensionality of Mack's first mode in 2-D boundary layers, whose most amplified disturbance is three-dimensional, crossflow in 3-D base flows results in three-dimensionality of stability characteristics in two folds. Firstly, the cross-wise perturbation velocity $\hat{w}$ is non-zero for zero cross-wise wave number β.

Secondly, the linear growths of disturbances with opposite wave angles are not identical with respect to the streamwise direction. The somewhat straightforward results are supported by the fact that asymmetry of eigen solution arises due to the appearance of crossflow. This fact can be inferred from the Symmetry Theorem below.

In a 2-D base flow (w=0), given $\left(\omega,\alpha,\beta,\phi\left(\hat{\rho},\hat{u},\hat{v},\hat{w},\hat{T}\right)\right)$ *as the solution of LST equation, a symmetric solution* $\left(\omega,\alpha,-\beta,\phi\left(\hat{\rho},\hat{u},\hat{v},-\hat{w},\hat{T}\right)\right)$ *exists. Especially if* $\beta=0$ *,* $\hat{w}=0$.

As a result, the stability characteristics, such as growth rate, wave angle and phase velocity, are symmetrically distributed with respect to β. This also implies that the disturbances pertinent to the symmetry solutions propagate with symmetric shape and identical growth rate in symmetric directions with respect to the streamwise direction. When crossflow plays a role in base flow, the proof of the theorem is ruined and consequently, the symmetry of the solution is broken. LST results about the asymmetry are demonstrated repeatedly in what follows.

RESULTS

Based on the base flow introduced above, spatial theory of viscous stability analysis is investigated. The boundary layer at Ma_e=4.5 is firstly considered to investigate the effects of crossflow on Mack's first and second modes, which are commonly encountered in 2-D conditions. The flow condition is chosen to be the one in wind tunnel (Kendall 1975), i.e., T_e^*=65.15K and unit Reynolds number $Re_e^*=7.2\times10^6\text{m}^{-1}$. The superscript '*' denotes the dimensional quantity and an adiabatic wall is assumed. This condition is also used by Ma & Zhong (2003) for boundary-layer stability analysis. The subscript 'e' will be dropped in what follows.

Basic characteristics of linear stability

Based on the knowledge of eigenmode in 2-D compressible boundary layers, global method (Malik 1990) is firstly used to identify the unstable mode from 2-D to 3-D conditions. Fig. 3 shows the spectra of eigen-values obtained with QZ algorithm. A discrete mode with positive growth rate is discovered for a 2-D boundary layer and highlighted by a circle in Fig. 3(*a*). The unstable mode is the well-known Mack's first mode, which is also the slow mode (Mode S) according to the terminology proposed by Fedorov & Tumin (2011). The result resembles the one obtained by Ma & Zhong (2003) except the fast mode (Mode F), which lies among the continuous spectra on the left of Fig. 3(*a*) and it is not discernible unless the frequency is moderately large. Eigen-value spectra are also obtained for 3-D boundary layers with crossflow by imposing pressure gradient and increasing local swept angle. Mode S is still found to be the only unstable mode in each case and its trajectory is illustrated in Fig. 3(*b*). Starting from the 2-D condition without and with pressure gradient, the mode travels away due to the appearance of crossflow. Based on such observations, Mode S is identified to be the target eigenmode for crossflow induced instability analysis. An iterative technique will be used to solve the eigen-value problem for higher efficiency, and the result obtained by global method can serve as a first guess.

The growth rate and phase velocity are calculated for 2-D mode (Fig. 4). Mack's first and second modes, both of which correspond to Mode S, locate obviously at two distinct frequency regions. This agrees with the result of Ma & Zhong (2003). Mack's second mode is observed to be more unstable than the first mode for 2-D disturbances, with and without the effect of crossflow. However, crossflow seems to stabilize both modes and shift the unstable frequency band in comparison with the 2-D boundary layers. Phase velocities are plotted for Mode S as well as Mode F in Fig. 4(*b*). Apparent deviation is observed for 2-D and 3-D base flows. While the local swept angle seems to make little effect on the phase velocity in 3-D base flows.

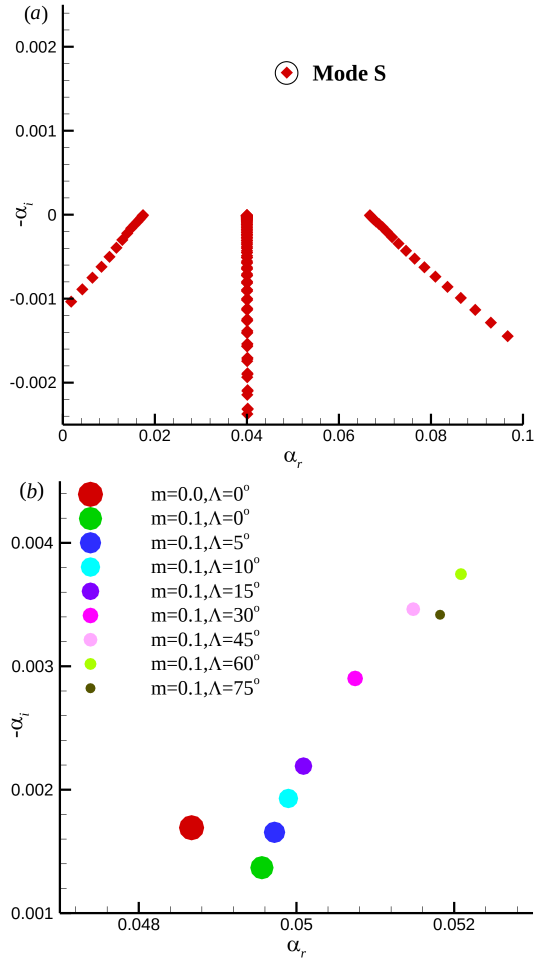

Figure 3. Eigen-value spectra for boundary layers with *Ma*=4.5, *Re*=2000, ω=0.04 and β=0.1. (*a*) Discrete and continuous spectra for a 2-D base flow. (*b*) Trajectory of Mode S for 3-D base flows.

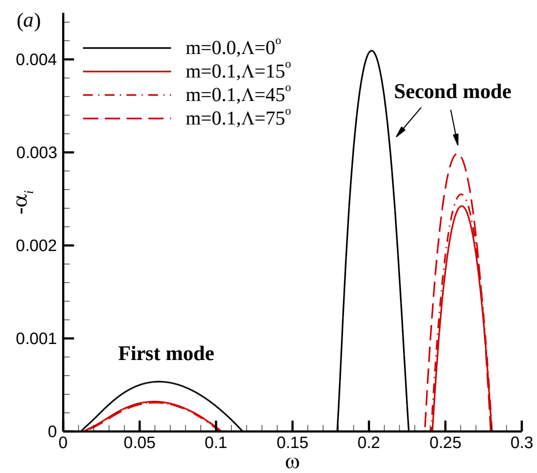

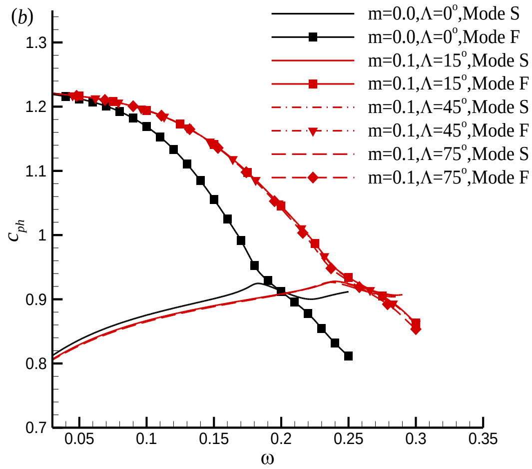

Figure 4. Distributions of (*a*) growth rate and (*b*) phase velocity against frequency for 2-D modes (*Ma*=4.5, *Re*=2000, β=0).

3-D stability characteristics are more concerned in boundary layers with crossflow. Based on the results of 2-D mode, eigen-value problems are solved for non-zero crosswise wave number, i.e., $\beta \neq 0$. The growth rate of Mode S is contoured in Fig. 5 at Λ=60°, around which the maximum of crossflow in base flow reaches the largest value. The result of a 2-D boundary layer (*m*=0.1, Λ=0°) is also presented for comparison. Two separate unstable regions with local maxima are observed and identified to be Mack's first mode and second mode, respectively. Symmetry in growth-rate distribution and negativeness in frequency are two marked features. For the 2-D base flow, the growth-rate distributions of Mack's first and second modes are strictly symmetric with respect to the horizontal line β=0, as shown in Fig. 5(a). The unstable regions of the first mode for positive and negative β coalesce. While the two regions are separate at lower Reynolds numbers with still symmetric distribution of growth rate. The result is in good agreement with the prediction of the Symmetry Theorem given above. Furthermore, the disturbance of crosswise velocity in 2-D base flow is zero for the first and second mode (Fig. 6), as predicted by the Symmetry Theorem.

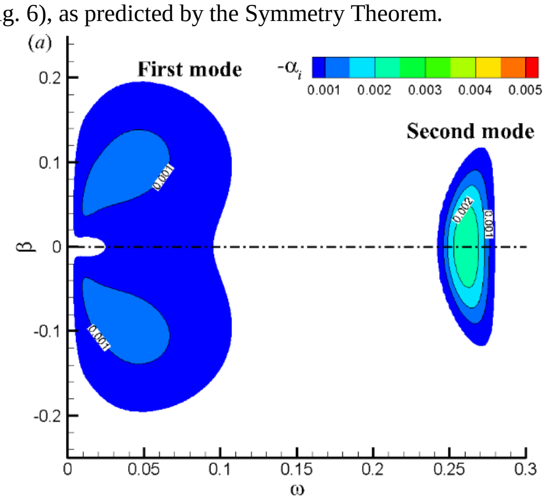

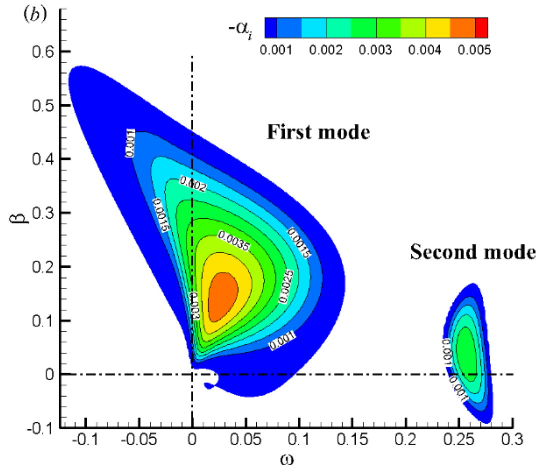

Figure 5. Growth-rate contours of the unstable modes in boundary layers (*Ma*=4.5, *Re*=2000, *m*=0.1) for (*a*) Λ=0° and (*b*) Λ=60°.

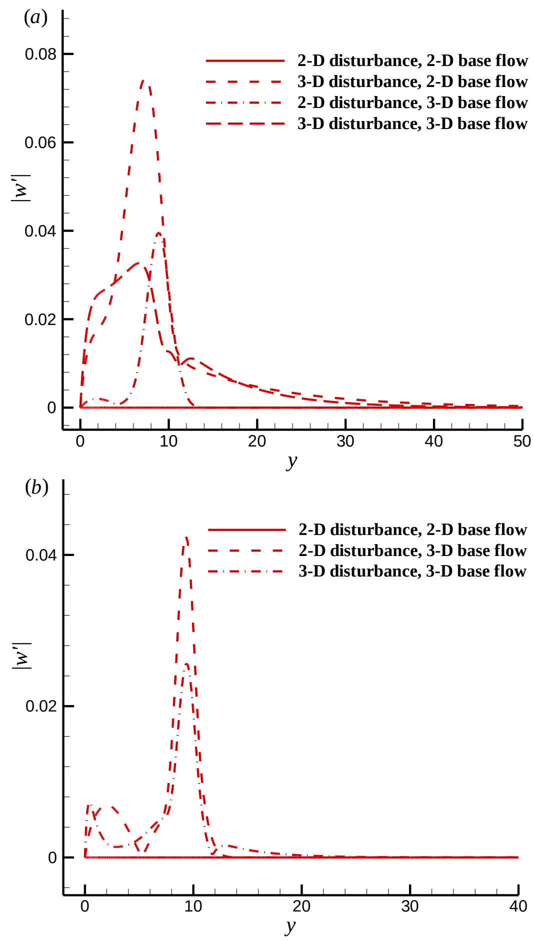

Figure 6. Distribution of disturbing crosswise velocity for 2-D and 3-D most amplified disturbance of the (*a*) first mode and (*b*) second mode. Λ=0° for 2-D base flow and Λ=60° for 3-D base flow (*Ma*=4.5, *Re*=2000, *m*=0.1).

In contrast, when crossflow plays a role in base flow, the symmetry is broken for both first and second modes. Meanwhile, the crosswise disturbing velocity becomes non-zero for 3-D disturbances in 2-D base flows, and for the 2-D and 3-D disturbances in 3-D base flows (Fig. 6). Under the effect of negative-value crossflow produced by favorable pressure gradient, the unstable regions move towards the direction in which β gets larger (Fig. 5(*b*)), i.e., opposite to crossflow direction. The asymmetry leads directly to the result that 3-D disturbance becomes the most amplified for the second mode, different from that in a 2-D boundary layer. More striking changes are observed for the first mode, whose unstable region is found to become almost one-sided. Firstly, the maximum growth rate exceeds that of the second mode, while the reverse is true in a 2-D case as demonstrated in Fig. 5(*a*). This implies that crossflow produces greater effect on the first mode than on the second mode. Secondly, the unstable frequency band of the first mode extends to comprise the zero and negative frequencies, which is unique in 3-D boundary layers. The zero-frequency unstable mode is the commonly encountered stationary cross-flow mode, and the more amplified disturbance with positive frequency is the traveling cross-flow mode. However, it is noted that the so-called cross-flow mode is no other than the slow mode, or Mack's first mode, depending on the terminology chosen. Crossflow in base flow does not essentially create a new unstable mode. Therefore, it seems more appropriate to name a stationary or traveling first mode rather than a cross-flow mode. This fact is supported by the numerical findings in a 3-D high-speed boundary layer presented by Xu *et al*. (2018). They obtained the disturbing crosswise velocity of Mode S, resembling the current result as shown in Fig. 6(*a*). It was illustrated that unstable traveling cross-flow wave can be evolved from Mode S upstream.

It might be argued that cross-flow mode is naturally qualified to name the unstable mode particularly induced by crossflow. Nevertheless, conventional usages of mode disagree with this argument. On the one hand, based on the terminology of Fedorov and Tumin (2011), the cross-flow mode is the solution related to Mode S. Thus, it cannot stand as a mode coequal to Mode S or Mode F. On the other hand, based on the terminology of Mack (1984), the cross-flow mode belongs to the deviated Mack's first mode. No distinguishable features are observed pertaining uniquely to cross-flow mode, if it exists. Thus, it cannot be a coequal mode as the first or second mode as well. Therefore, cross-flow mode is less appropriate to signify the crossflow-induced unstable mode. This viewpoint will gain more support from stability analysis in the following subsections.

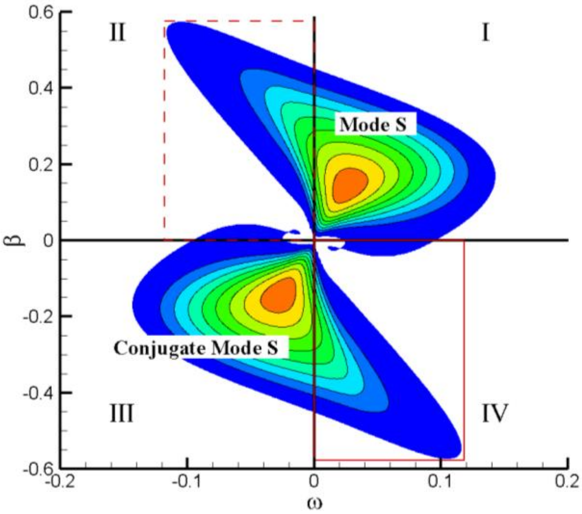

Figure 7. Growth-rate contour of conjugate modes (Mode S, Ma=4.5, Re=2000, m=0.1, Λ=60°).

With the increase of cross-flow strength in base flow, the unstable region of the first mode deviates from that shown in Fig. 5(*a*). For weak crossflow, stationary mode stays stable. When the maximum of crossflow exceeds a threshold value (around 0.012 under such condition), stationary first mode begins to be unstable. At even larger cross-flow strength, the stationary first mode gets more unstable with broader bandwidth of crosswise wave number, and negative-frequency disturbances become unstable as well, as shown in Fig. 5(*b*). According to the Conjugate-Solution Theorem presented above, a conjugate solution can be easily obtained based on a known solution by turning the parameters into their negative and conjugate counterparts. Fig. 7 shows the growth-rate contours of Mode S as well as the conjugate Mode S. The contours are rotationally symmetric, while the two modes are related to different eigen solutions. Thus, the growth-rate contours cannot connect with each other continuously. The plane in Fig. 7 is divided into quadrant I, II, III and IV. The unstable wave of Mode S with negative frequency are surrounded with dashed lines in quadrant II, and the counterpart surrounded with solid lines in quadrant IV bears positive frequency. Therefore, when the negative-frequency mode needs to be considered, a more physical choice is to consider its conjugate mode with positive frequency and opposite wave numbers. The puzzle of negative-frequency mode is thus solved by resorting to the conjugate mode. In addition, as the usually-encountered unstable wave of Mode S in quadrant I has positive frequency, its conjugate mode in quadrant III is far less concerned. Exceptions may be encountered in boundary layers with adverse pressure gradient. In such cases, the negative-frequency unstable region is stretched from quadrant IV to quadrant III, thus the counterpart in quadrant I is worth consideration. It is also observed that, despite the rotational symmetry of conjugate modes, symmetry with respect to crosswise wave number does not exist. This indicates that the distributions of growth rate and unstable crosswise-wavenumber band are not symmetric for a given disturbance, unless its frequency is zero. The current results combined with the Conjugate-Solution Theorem, provides an alternative approach to understand and treat negative-frequency mode. The understanding is in accordance with that of Mack (1984) and Itoh (1996). However, evidence has long been absent until it is supplemented theoretically in current work.

It should be noted that conjugate mode is significant in 3-D boundary layers regardless of Mach numbers. Borodulin *et al*. (2019) measured experimentally the unsteady cross-flow instability in incompressible boundary layers on a swept airfoil. The crosswise-wavenumber spectra reveal two unstable modes for a given positive frequency. The mode with negative crosswise wave number is named Mode 1 therein, and the other Mode 2. The Mode 1 has smaller growth rate and narrower unstable crosswise-wavenumber bandwidth. Besides, the two modes exhibit symmetry only for quasi-stationary disturbances. Based on such observations, it is believed that the Mode 2 is the cross-flow mode, as called in that paper, and the Mode 1 is the conjugate mode.

The boundaries of growth-rate contours are extracted to denote unstable regions and plotted in Fig. 8(a) for various Reynolds numbers. The unstable region enlarges along with the increase of Reynolds number, and the stationary disturbance emerges at a Reynolds number of around 400. At moderately small Reynolds numbers, the unstable region of the first mode is completely one-sided. The maximum growth rates and corresponding wave angles are calculated for the first and second modes. The 2-D and 3-D results are plotted for comparison, as shown in Fig. 8(b) and Fig. 8(c). The growth rates of both modes are found to increase with Reynolds number in a 3-D boundary layer, which indicates a stabilizing effect of viscosity as in a 2-D case. Thus, the crossflow seems not to alter the viscous effect. While the crossflow does change the specific instability characteristics, like growth rate and wave angle. Apparent discrepancies in maximum growth rate are observed for both modes (Fig. 8(b)). The first-mode growth rate in a 3-D base flow is unanimously larger than that in a 2-D base flow. The reverse is true for the second mode. The contrary effects mean that the first mode is destabilized, while the second mode is stabilized by crossflow. Consequently, the first mode becomes more unstable than the second mode in a broader Reynolds-number range. In addition, the most amplified disturbances for both modes are found to propagate in more tilted directions under the effect of crossflow. The wave angle of the second-mode disturbance with maximum growth rate varies between 4o and 5o, compared with the exact 0o in a 2-D case. This result quantitatively reveals the asymmetry of the second mode as discussed previously.

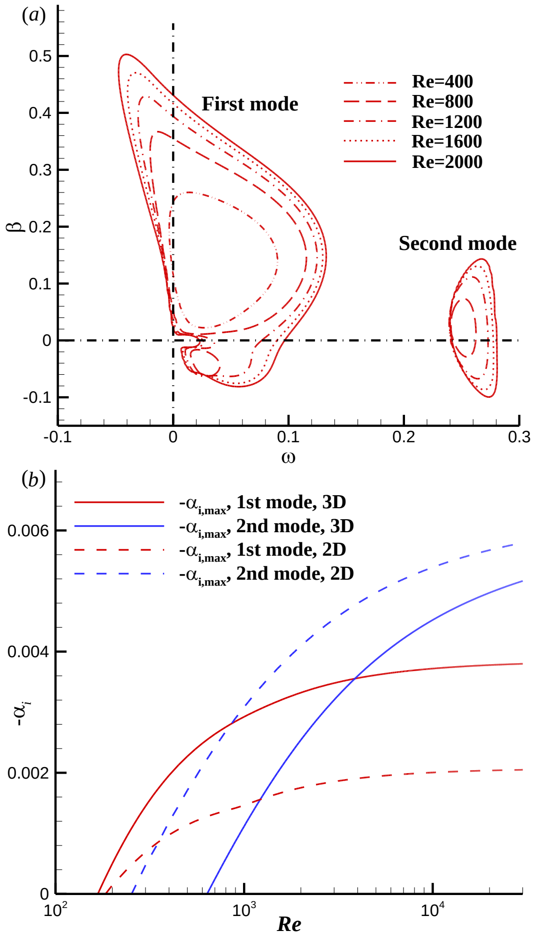

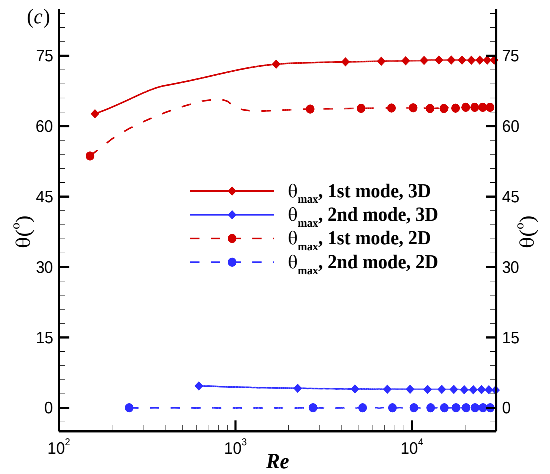

Figure 8. Characteristics of unstable modes at various Reynolds numbers (Ma=4.5, Λ=30°, T_w=T_{ad}). m=0.1 for 3-D base flows and m=0 for 2-D base flows. (*a*) Unstable ω-β region; (*b*) Maximum growth rate; (*c*) Wave angle.

Inconsistency can be observed about the effect of crossflow on second mode by comparing Fig. 8 with Fig. 5. Under the effect of crossflow, the second-mode maximum growth rate in a 3-D boundary layer is higher in Fig. 5, while lower in Fig. 8, than that in a 2-D boundary layer. This is because the 2-D base flow is subject to a favorable pressure gradient in Fig. 5, compared with the absence of pressure gradient for the 2-D base flow in Fig. 8. Accompanied by imposing an additional local swept angle Λ to create crossflow, the streamwise pressure gradient parameter decreases to $m\cos\Lambda$ in Fig. 5. As pointed out by Zurigat, Neyfeh & Masad (1992), a streamwise favorable pressure gradient has a stabilizing effect on the second mode in a 2-D compressible boundary layer. According to this fact, decreasing favorable pressure gradient in streamwise direction suggests the increasingly unstable second mode, as shown in Fig. 5. In contrast, increasing streamwise pressure gradient is imposed to produce crossflow in Fig. 8, thus an decrease in second-mode growth rate is observed.

Effects of Mach number

In 2-D boundary layers, the behaviors of the first and second modes are well-known at varying Mach numbers. The first mode, which reduces to T-S wave in subsonic flows (Fedorov 2011), exists in whole range of Mach number. In comparison, the second mode appears when Ma>2.2 and becomes dominant in hypersonic flows. However, limited understanding has been recognized about the crossflow-affected instabilities in 3-D compressible boundary layers. In this section, we investigate the Mach number effect on the stability in boundary layers with crossflow.

The incompressible boundary layer is firstly considered by setting Mach number to be 0.001. As mentioned above, the base flow in current model reduces to FSC flow when Mach number approaches zero. At such low Mach numbers, Mack's second mode is not expected. In contrast, the T-S wave, which is more often termed as T-S mode or the first mode in this paper, is the main concern. In order to reveal the increasing effect of crossflow, a 2-D base flow is preliminarily considered and crossflow is added gradually. Fig. 9 shows the growth-rate contours for different local swept angles, corresponding to the cross-flow maximum of 0, 0.013 and 0.034 respectively. Starting with the use of global method, the unstable modal solution is found to be related with Mode S for all three cases. In a 2-D base flow, the growth rate of T-S mode is symmetrically distributed (Fig. 9(*a*)), and the most amplified wave is 2-D as reported by Mack (1984). Apart from the T-S mode, a new unstable region arises with the increase of crossflow, as shown in Fig. 9(*b*). Again, the asymmetry of growth-rate distribution for T-S mode is observed due to crossflow. Despite the seeming disconnection of the two unstable regions, they belong to a common solution, thus they are actually connected by the stable region in between. The newly emerging unstable region bears lower frequency, higher growth rate and larger crosswise wave number than the T-S mode region. By comparing with Mack's (1984) result about FSC boundary layers, it can be identified that this region corresponds to cross-flow instability. At even stronger crossflow, the two unstable regions coalesce, accompanying with the decrease on the number of peaks from two to one (Fig. 9(*c*)). The cross-flow instability and the T-S instability cannot be distinguished in this case.

The appearance of cross-flow instability at *Ma*=0.001 differs strikingly from the crossflow-affected instability at *Ma*=4.5 as shown in the preceding subsection. In the highly supersonic boundary layers with crossflow, Mack's first mode deviates to exhibit some characteristics of cross-flow instability, despite that the cross-flow instability can hardly be distinguished. While in the incompressible boundary layers, crossflow produces an additional cross-flow instability competing with T-S instability. The cross-flow instability occupies a separate unstable region at a moderate strength of crossflow. A local maximum of growth rate always exists for cross-flow instability, corresponding to the most amplified traveling cross-flow wave. Although the T-S mode becomes fairly more unstable with the increase of crossflow, the intensity of cross-flow instability grows even more sharply. Finally, the unstable region of cross-flow instability enlarges and swallows that of T-S instability.

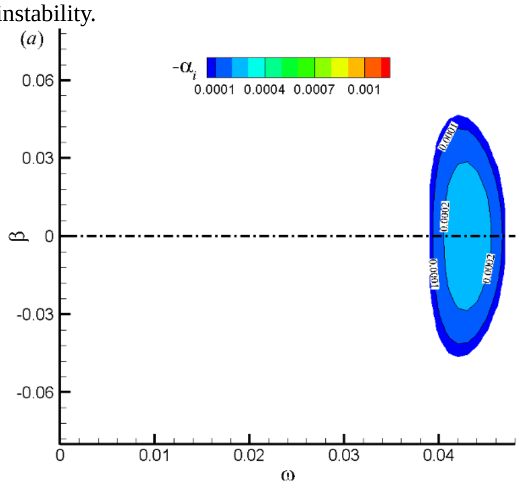

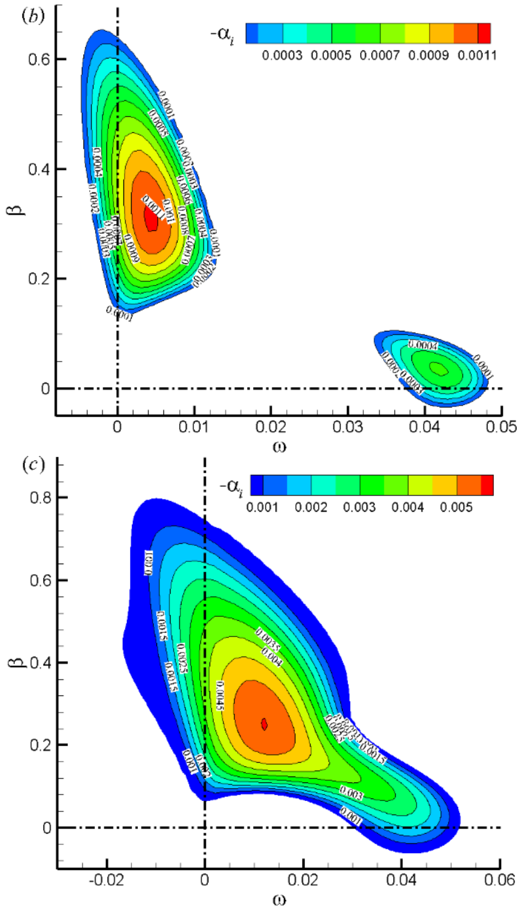

Figure 9. Growth-rate contours of the unstable modes in incompressible boundary layers for (*a*) $\Lambda=0^{o}$, (*b*) $\Lambda=10^{o}$ and (*c*) $\Lambda=30^{o}$ (m=0.1, Re=2000).

The growth-rate distributions are contoured for unstable modes in compressible boundary layers at various Mach numbers in Fig. 10. The result in each case is obtained by increasing gradually the strength of crossflow from zero. Thus, the presented instabilities can be traced and identified based on 2-D results. Under such moderate strength of crossflow, the intensities are comparable for different instabilities, if there exists more than one instability in the case. Cross-flow modes are shown for cases with Mach numbers less than 1.5. While for larger Mach numbers, the cross-flow instability cannot be distinguished to be a mode, as discussed previously. The cross-flow mode and T-S mode get entangled at *Ma*=1.0 (Fig. 10(b)), and the mode entanglement is also observed for the first mode and second mode at *Ma*=6.0 (Fig. 10(f)).

The name of cross-flow mode is usually encountered in incompressible and compressible boundary layers. However, current results reveal that the cross-flow instability cannot be recognized as an individual mode in most cases. The phenomenal similarity underpins the proposition of naming the cross-flow instability as a mode at low speeds. However, is should be borne in mind that the cross-flow instability is integrated in the T-S mode or the first mode. Particularly in highly supersonic boundary layers, the usage of cross-flow mode is ambiguous.

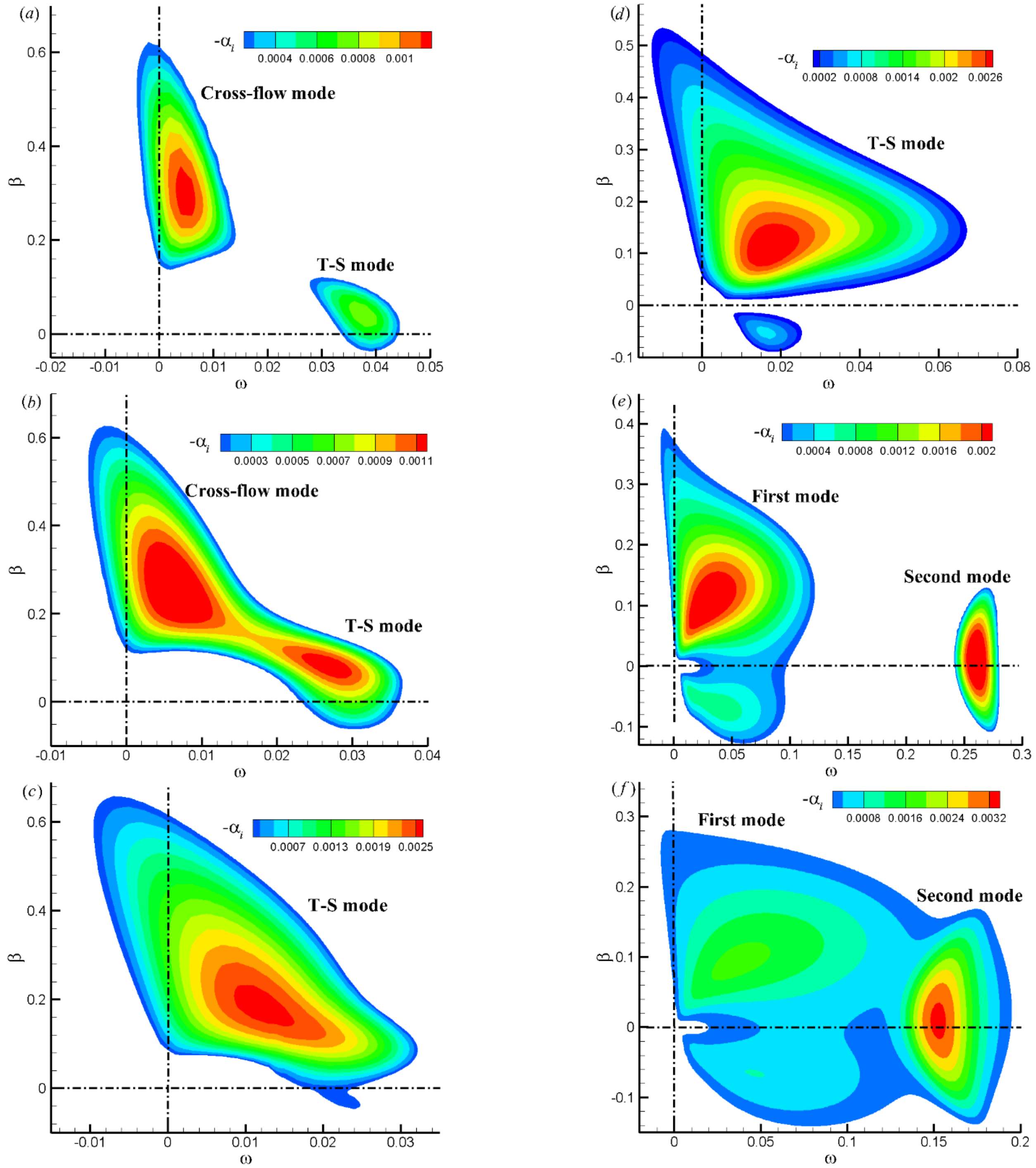

Figure 10. Growth-rate contours of the unstable modes in compressible boundary layers (Re=2000, m=0.1, T_w=T_{ad}) with (a) Ma=0.5, Λ=10°; (b) Ma=1.0, Λ=10°; (c) Ma=1.5, Λ=15°; (d) Ma=3.0, Λ=15°; (e) Ma=4.5, Λ=15° and (f) Ma=6.0, Λ=15°.

CONCLUDING REMARKS

The stability characteristics of 3-D boundary layers subject to parametric crossflow have been investigated. A base-flow model on a flat plate is firstly designed to create boundary layer with crossflow. Considering that the crossflow is intrinsically resulted from crosswise pressure gradient, potentially fewest parameters, i.e., pressure-gradient parameter and local swept angle, are chosen to parameterize crossflow in the model. The model base flow is governed by an ODE system, which permits local similarity for the boundary layer.

Using the proposed model, we obtained a family of 3-D boundary layer, which can be reduced to the incompressible FSC flow and 2-D compressible self-similar boundary-layer flow. Based on such base flows, we extended the stability analysis from in 2-D cases to in 3-D cases at various Mach numbers.

Asymmetry and negativeness of frequency are found to be fundamental features for cross-flow instability in 3-D boundary layers. Two theorems, i.e., Symmetry Theorem and Conjugate-Solution Theorem are primarily proposed to reveal the intrinsic details. Both theorems have been proved theoretically and numerically. The symmetric distributions of stability characteristics in 2-D flows are demonstrated by Symmetry Theorem and LST results. The occurrence of instability asymmetry in a 3-D flow is believed to be attributed to crossflow, whose existence ruins the symmetry of the base flow. The occurrence of negative-frequency disturbance is revealed repeatedly in the results of stability analysis. According to Conjugate-Solution Theorem, a conjugate solution with positive frequency exists for a negative-frequency solution. Therefore, although the negative-frequency disturbance *per se* is notorious for lack of physical meaning, its conjugate counterpart is suggested to be resorted to for physical applications. Meanwhile, the Conjugate-Solution Theorem further indicates opposite propagating directions for the negative- and corresponding positive-frequency disturbances, which is accordant to what has been suppositionally recognized.

Based on a large number of calculations, it is revealed that the occurrence of crossflow does not essentially create a new discrete solution. All of the LST solutions obtained in this paper are found to be related to Mode S, according to the mode terminology proposed by Fedorov and Tumin (2011). However, the crossflow does give rise to different behaviors of Mode S from those in 2-D boundary layers. The differences are in two folds. Firstly, the cross-flow instability, which is characterized as containing zero and negative frequency band, emerges. And it is found to be integrated in T-S mode at low Mach numbers or the first mode at high Mach numbers. The cross-flow instability can hardly be identified as an individual mode for most cases, even based on a loose definition of mode like Mack's first and second mode. But exceptions are found to exist for moderate crossflow in favorably pressure-gradient boundary layers with Mach number less than 1.5. Secondly, the crossflow seems to destabilize the T-S/first and second modes in general, by expanding unstable regions and increasing growth rates. Meanwhile, the unstable modes become more oblique towards crosswise or the opposite direction, depending on favorable or adverse pressure gradients. In comparison, the first mode is much more greatly affected by crossflow than the second mode.

REFERENCES

Balakumar, P. & KIing, R. A. 2012, "Receptivity and stability of supersonic swept flows." *AIAA Journal.* 50(7), 1476-1489.

Borodulin, V. I., Ivanov, A V., Kachanov, Y. S., Mischenko, D. A., Örlü, R., Hanifi, A. & Hein, S. 2019, "Experimental and theoretical study of swept-wing boundary-layer instabilities. Unsteady crossflow instability," *Physics of Fluids*. 31(6): 064101.

Cooke, J. C., 1950, "The boundary layer of a class of infinite yawed cylinders," *Mathematical Proceedings of the Cambridge Philosophical Society,* 46(4), 645-648.

Corke, T. C., Arndt, A., Matlis, E. & Semper, M. 2018, "Control of stationary cross-flow modes in a Mach 6 boundary layer using patterned roughness," *Journal of Fluid Mechanics,* 856, 822-849.

Craig, A. S. & Saric, W. S. 2016, "Crossflow instability in a hypersonic boundary layer," *Journal of Fluid Mechanics,* 808, 224–244.

Dinzl, D. J. & Candler, G. V. 2017, "Direct simulation of hypersonic crossflow instability on an elliptic cone," *AIAA Journal,* 55(6), 1769-1782.

Fedorov, A & Tumin, A. 2011, "High-speed boundary-layer instability: old terminology and a new framework," *AIAA Journal.* 49(8), 1647-1657.

Högberg, M. & Henningson D. 1998, "Secondary instability of cross-flow vortices in Falkner-Skan-Cooke boundary layers," *Journal of Fluid Mechanics,* 368, 339–357.

Itoh, N. 1996, "Simple cases of the streamline-curvature instability in three-dimensional boundary layers," *Journal of Fluid Mechanics,* 317, 129-154.

Kendall, J. M. 1975, "Wind tunnel experiments relating to supersonic and hypersonic boundary-layer transition," *AIAA Journal*. 13(3): 290–299.

Li, F., Choudhari, M., Paredes, P., and Duan, L., 2016, "High-frequency instabilities of stationary crossflow vortices in a hypersonic boundary layer", *Physics Review of Fluids*, 1: 053603.

Liu, Z. 2021, "Compressible Falkner-Skan-Cooke boundary layer on a flat plate," *Physics of Fluids*, 33, 126109.

Ma, Y. & Zhong, X. 2003, "Receptivity of a supersonic boundary layer over a flat plate. Part 1. Wave structures and interactions," *Journal of Fluid Mechanics,* 488, 31–78.

Ma, Y., and Zhong, X., 2005, "Receptivity of a supersonic boundary layer over a flat plate. Part 3. Effects of different types of free-stream disturbances", *Journal of Fluid Mechanics*, Vol. 532, pp. 53–109.

Mack, L. M., 1984, "Boundary-layer linear stability theory", AGARD Report No. 709, Special Course on Stability and Transition of Laminar Flow.

Malik, M. R., Li, F. & Chang, C.-L. 1994, "Crossflow disturbances in three-dimensional boundary layers: nonlinear development, wave interaction and secondary instability," *Journal of Fluid Mechanics,* 268, 1-36.

Malik, M. R., Li, F., Choudhari, M. M. & Chang, C.-L. 1999, "Secondary instability of crossflow vortices and swept-wing boundary-layer transition," *Journal of Fluid Mechanics,* 399, 85-115.

Paredes, P., Gosse, R., Theofilis, V., and Kimmel, R., 2016, "Linear modal instabilities of hypersonic flow over an elliptic cone", *Journal of Fluid Mechanics*, Vol. 804, pp. 442-466.

Pruett, C. D., Chang, C.-L. & Streett, C. L. 2000, "Simulation of crossflow instability on a supersonic highly swept wing," *Computers and Fluids,* 29, 33-62.

Saric, W. S., Reed, H. L., and White, E. B., 2003, "Stability and transition of three-dimensional boundary layers", *Annual Review of Fluid Mechanics*, Vol. 35, pp. 413-440.

Schrader, L.-U., Brandt, L. & Henningson, D. S. 2009, "Receptivity mechanisms in three-dimensional boundary-layer flows," *Journal of Fluid Mechanics*, 618, 209-241.

Schuele, C. Y., Corke, T. C. & Matlis, E. 2013, "Control of stationary cross-flow modes in a Mach 3.5 boundary layer using patterned passive and active roughness," *Journal of Fluid Mechanics,* 718, 5-38.

Stewartson, K., 1964, "The theory of laminar boundary layers in compressible fluids," Oxford: Oxford University Press.

Tempelmann, D., Hanifi, A. & Henningson, D. S. 2012, "Spatial optimal growth in three-dimensional compressible boundary layers," *Journal of Fluid Mechanics*, 704, 251-279.

Wassermann, P. & Kloker, M. 2002, "Mechanisms and passive control of crossflow-vortex-induced transition in a three-dimensional boundary layer," *Journal of Fluid Mechanics*, 456, 49–84.

Wassermann, P. & Kloker M. 2003, "Transition mechanisms induced by travelling crossflow vortices in a three-dimensional boundary layer," *Journal of Fluid Mechanics*, 483, 67–89.

White, E. B. & Saric, W. S. 2005, "Secondary instability of crossflow vortices," *Journal of Fluid Mechanics*, 525, 275-308.

Xu, G., Chen, J., Liu, G., Dong, S. & Fu, S. 2019, "The secondary instabilities of stationary cross-flow vortices in a Mach 6 swept wing flow," *Journal of Fluid Mechanics*, 873, 914–941.

Xu, G., Chen, J., Liu, G., and Fu, S., 2018, "Role of freestream slow acoustic waves in a hypersonic three-dimensional boundary layer", *AIAA Journal*, Vol. 56, No. 9, pp. 3570–3584.

Zurigat, Y. H., Nayfeh, A. H. & Masad, J. A. 1992, "Effect of pressure gradient on the stability of compressible boundary layers," *AIAA Journal.* 30(9), 2204–2211.